Reflex Assisted Walking for a Hexapod Robot

S.T. Marais
Department of Mechanical and Industrial Engineering
University of Johannesburg
South Africa
Email:stephentmarais@gmail.com

A.L. Nel
School of Mechanical and Industrial Engineering
University of Johannesburg
South Africa
Email: andren@uj.ac.za

P.E. Robinson
Department of Electrical and Electronic Engineering
University of Johannesburg
South Africa
Email: philipr@uj.ac.za

***Abstract*—This paper describes the performance of a hexapod robot that uses low level leg reflexes to aid in walking over uneven terrain, and is currently being developed at the University of Johannesburg. The goal of this research is a robot able to deploy in both the inspection and search and rescue roles, within an underground mine environment. The robot has six legs with three degrees of freedom per leg, and is equipped with a two degree of freedom arm with a sensor payload attached to a pan-tilt system. Throughout the development of this new robot the Design Science Research Methodology was used to guide the decision making process. This paper presents an overview of the robot, including the control architecture, and the testing conducted to verify the robot's performance when walking over a laboratory test field.**

I. Introduction

In the event of a natural or man-made disaster the first responders have to risk their lives when entering the disaster site. The ability of a robotic system to first enter and assess the disaster site, before a first responder enters, would reduce this risk [1]. The ability of the robotic system to provide essential data about the disaster site can also aid in the decision making process. This was demonstrated following the attacks on the World Trade Centre in the United States, when small robotic systems were sent into sections of the collapsed buildings to search for survivors [2][3][4]. More recently at the Fukushima nuclear power plant disaster in Japan (2011), robotic systems provided valuable data about the state of the nuclear reactor after the incident [5].

The need to reduce the risk to humans is not limited to natural or man-made disasters in urban areas, but is equally relevant in the mining sector in South Africa. In the event of an explosion or a tunnel collapse in a mine, a robot could conceivably be deployed to assess the air quality, determine the structural integrity of the tunnel, and search for survivors. In addition, the robotic system could produce accurate 3D maps of the tunnels and the collapsed areas. Providing the rescuers and mine engineers with data on how to proceed with the rescue operation, and what equipment and resources would be needed.

Reducing the risk to humans is not only limited to a disaster in a mine but in the everyday operation of the mine. After drilling, placing the explosives and finally detonating a charge, a safety officer has to enter this newly blasted area of the mine and assess its safety. The potential for injury is high as there are loose overhead rocks that must first be removed or secured. Currently, the instrumentation to scan the mined area has to be carried to just outside the newly blasted area, the sensor is then set up and the necessary data collected. Not being able to enter the newly blasted area restricts the range of the scans and limits the view point. A robotic system could aid this process by being able to transport the sensor payload into the restricted area and take readings from multiple viewpoints without the risk to humans.

For both the search and rescue scenario and the routine inspection role, the robotic system required to enter this harsh environment faces the challenge of navigating and traversing very uneven terrain [6][7].

The remainder of this paper is structured as follows. In the next section the past work that leading to this robot design is discussed. A description of the layout of the robot follows, and includes the control architecture used to operate the robot. The testing of the robot's ability to walk over uneven terrain, and the conclusions drawn are then presented.

II. Background to the Robot Design

The work described in this paper is a continuation of the work carried out on a robot developed at the Robotics and Agents Research Lab (RARL), at the University of Cape Town, by Booysen and Marais [8]. The RARL robot had a limited payload capacity, and the physical size limited the object that could be stepped over or climbed. The robot used the ROBOTIS™ Dynamixal™ RX-28 servo motors on each leg joint. These motors produce a stall torque of $2.5\ Nm$ when run at $12\ V$, and there was limited scope to add a sensor arm to the robot without overloading the leg motors.

The new robot, described in this paper, was designed to be 50% larger than its predecessor, and uses Dynamixal™ MX-106 servo motors, with a stall torque of $8.8\ Nm$ at $12\ V$. A sensor arm was designed to allow the sensor payload to be raised up $500\ mm$ above the robot body so that the RGB-D cameras could get a better view of the terrain. The arm could also move in front of the robot to see over obstacles that the robot would encounter, and have sufficient movement to look under the robot body if needed. Throughout the development of this new robot the Design Science Research Methodology (DSRM) [9] was used to guide the decision making process.

III. Robot Layout

The hexapod robot was designed with the legs equally spaced at 60° at a distance of 187.5 mm from the centre of the robot to the centre of the shoulder pan motor. A CAD rendering of the robot base and sensor arm without the controller is shown in Fig. 1.

Fig. 1. CAD rendering of the robot base with sensor arm

Each leg has 3 DOF, with 2 motors at the shoulder joint and one at the knee joint. All three motors for the leg are ROBOTIS™ Dynamixal™ MX-106 servo motors. A CAD rendering of a leg, and a skeletal view with dimensions is shown in Fig. 2

The sensor arm was designed to be a two-link arm with a pan-tilt system at the end effector. The base and elbow joints are driven by Dynamixal™ MX-106 servo motors, with the tilt and pan joints driven by Dynamixal™ MX-28 servo motors. The sensor payload for this phase of the project is a Xtion PRO LIVE. A CAD rendering of a sensor arm with the sensor payload is shown in Fig. 3 a) and a skeletal view with dimensions for the arm in b).

IV. Control Architecture

To operate the robot and send it instructions, the operator has the selection of using a Game Pad or a menu interface. Both the Game Pad and the menu run on the Base Station PC, and this PC operates using the Robot Operating System (ROS). The Base Station then communicates with the robot via a TCP/IP link. On the robot, the high level processing is done on a FitPC-Intense PC with an Intel 3rd Gen Core i7 Quad Core, 1.7 GHz with 16 GB RAM running ROS. This processes the point cloud data from the Xtion PRO LIVE, generates the walk pattern, and calculates the robot coordinates for the step sequence. The step sequence for each step is broken into 40 individual parts, and at each of these the coordinates for the robot are determined using inverse kinematics with the vector mechanics method [10]. When the coordinates of the robot joints are determined a robot model integrity check is carried out. If these checks pass, then arrays of the robot coordinates are then passed to a National Instruments (NI) myRio Real Time (RT) controller via a TCP/IP link. This controller is responsible for running the control for all of the

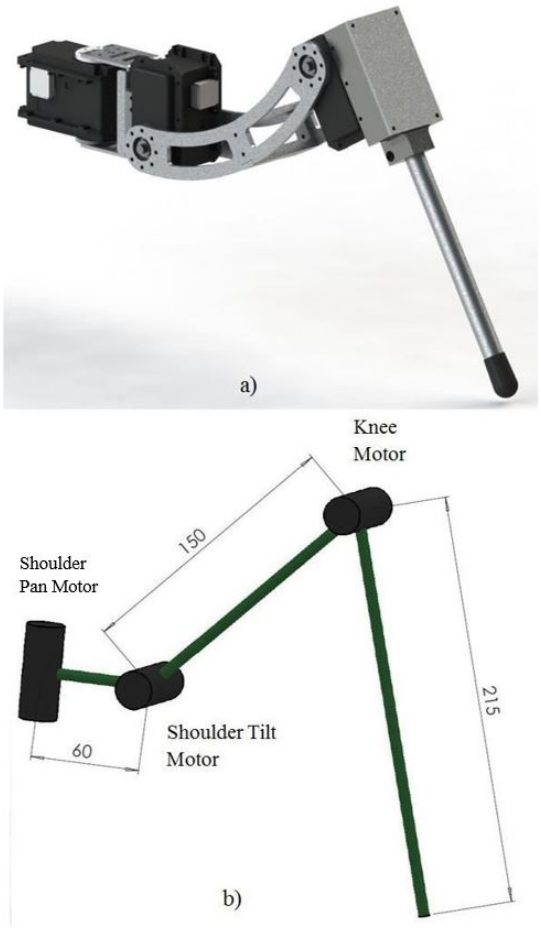

Fig. 2. a) CAD rendering of leg. b) Skeletal view of leg with dimensions

robot's 22 motors. This architecture is similar to that used by the Aldebaran Nao robot [13] and the HITCR-II [14]. Figure 4 shows a block diagram of the four components making up the control architecture of the robot.

The myRio RT controller has two main functions. The first is to run the motors deterministically and to run the low level leg reflexes. These reflexes will be described in more detail below. The second function is to monitor all aspects of the robot's performance and decision making process, and then transmit this data via WiFi to a system monitoring and data logging PC.

When walking over unstructured terrain three low level leg reflexes are utilised to position or reposition the legs while walking. These leg reflexes operate at the lowest level of control and required no input from the PC running ROS. Utilising these three legs reflexes the robot is capable of making its way over uneven terrain without the use of any type of visual sensors, i.e. blind walking. These leg reflexes are based on the work done by Espenschied et al. [11] which used load sensors to detect a leg contact, and the work by Mrva and Faigl [12] with used the positional data from the motors. This work expands on this and only the loading data from the motors was used to detect if a leg has made contact.

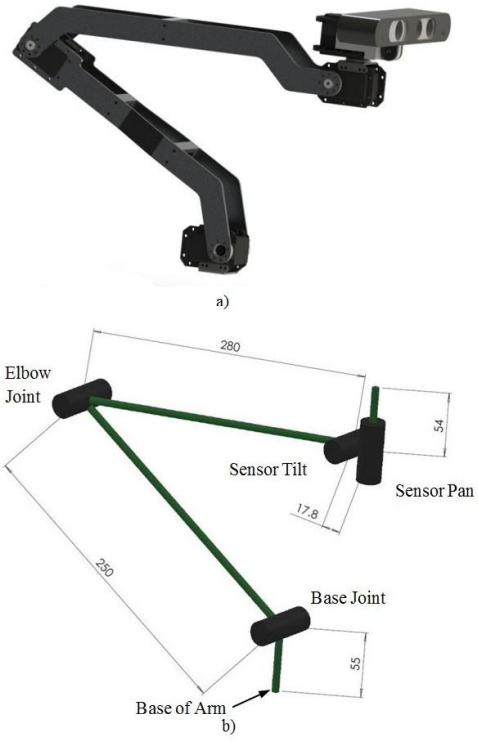

Fig. 3. a) CAD rendering of the sensor arm b) Skeletal view of the sensor arm with dimensions

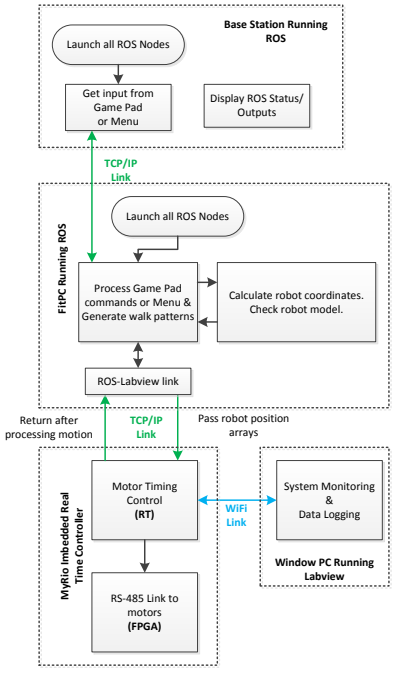

Fig. 4. Control Architecture and Data Flow

A. Seek Down Reflex

The Seek Down reflex, which is the simplest of the three reflexes, is called to drive a leg vertically down at the end of a step sequence if the leg is not loaded. The leg is driven down until the robot leg loading system determines that the leg is carrying sufficient load to support the robot.

B. Touch Reflex

The Touch reflex is the main reflex that deals with repositioning a leg, once it has been determined to have made contact with an object. The Touch reflex deals with two main leg contact situations. The first is when a foot makes contact with a level surface before the end of the step phase, and the second is when a leg makes contact with the side of an object.

C. Lost Footing Reflex

The final reflex repositions a foot after it has lost footing, and is no longer carrying a support load. The Lost Footing reflex deals with two situations. The first is when a foot is on the ground, but not carrying sufficient support load. This condition predominately occurs when all the feet are in contact with the ground and the robot is transitioning from one leg set to another. The second situation occurs when the leg is positioned too close to an edge, the robot shifts its mass, and the leg slips off the object. In this condition, the reflex goes into a search sequence to find a footing for the leg.

V. Step Trajectory

The foot trajectory used for testing is made up of four sections. The start and end sections are a vertical move up and a vertical move down, respectively. These sections are relatively small in comparison to the overall step height, and functions to eliminate scuff when walking on soft surfaces such as carpet, sand and grass. The foot first moves up before any horizontal movement is initiated. The next two sections are separate and sinusoidal. The first sinusoidal section starts at the end of the first vertical rise and ends at the midpoint of the step, or at the maximum point of the step. The second sinusoidal section starts at the midpoint of the step and ends at the start of the vertical down section.

For the step trajectory there are three scenarios to be dealt with. The first applies to the start and end heights of steps taken on the same level, and in this case, the step height is set to a clearance distance of 30 mm. The second case applies when the leg is stepping up onto an object. In this case the difference between the end step height and start step height is calculated, with a clearance distance of 30 mm added to the difference. This value is then used as the step height. The addition of the 30 mm to the step height is to ensure that the foot clears the obstacle and the step trajectory is in the downward phase of the step before making contact with the obstacle. The last scenario applies to a leg stepping down from an obstacle, and in this case the step height is set to the 30 mm clearance distance. The trajectories for stepping up onto an obstacle and down from an obstacle are shown in Figure 5 a) and b), respectively.

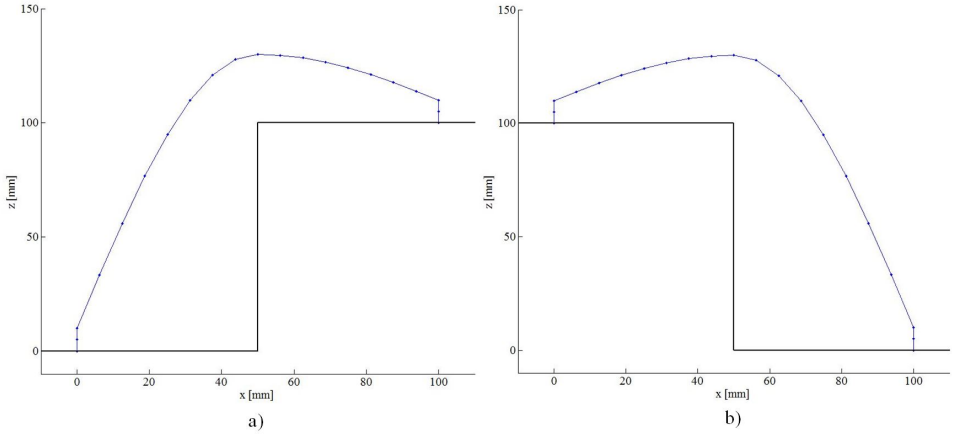

Fig. 5. Step trajectories for a foot stepping onto an obstacle a), and from an obstacle b)

VI. Testing

A. Stepfield Setup

The simulated disaster site used to test the performance of the robot was constructed in accordance to a NIST setpfield, with the exception that the block heights could be altered in increments of 12 mm. The blocks that make up the different obstacles in the test arena were manufactured by laminating 100 mm by 100 mm tiles cut from 12 mm thick high-density fiberboard. The layout of the stepfield is such that each leg entering encounters a block of different height. With the overall effect being that as many legs as possible, within the stepfield, are at differing elevations. The layout of the stepfield and starting position of the front two legs are shown in Figure 6.

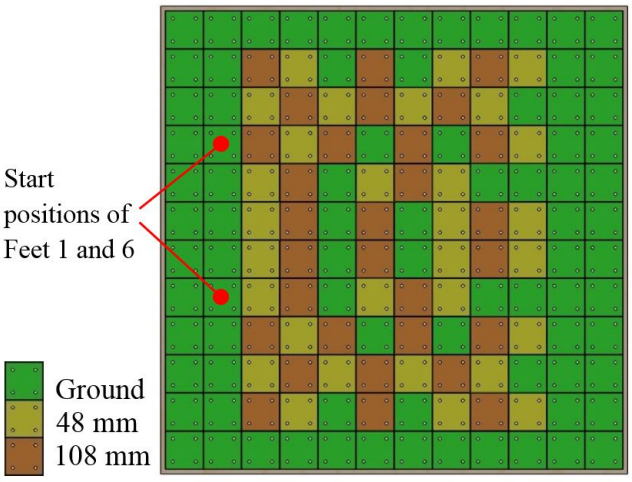

Fig. 6. Plan view of the test cell configured as a stepfield

B. Preliminary Blind Walking Testing

To test that the robotic system and the leg reflexes were functional, several tests were conducted. For all these tests no vision assistance was used to determine the terrain ahead of the robot. The robot was in effect blind and had to feel its way across or over the terrain ahead. The tests included having the robot walk over a level surface at different body ride heights, walk up an incline up to 20°, climb over an obstacle, and walk up stairs. The final test required the robot to make its way over an unstructured stepfield.

C. Vision Assisted Testing

Having completed the blind testing and demonstrated that the system was functional, the vision system was incorporated into the robot's control system. The robot then tackled the stepfield with the aid of data from the RGB-D camera. For the start of the test the robot was placed in the default standing position (Figure 7 a)) and the two front feet (Foot 1 and 6) were positioned 50 mm from the edge of the first row of stepfield blocks. The robot was instructed to move to the scan position, shown in Figure 7 b), and to take the five scans needed for a complete image of the stepfield. After the scans were completed the robot was returned to the default standing position. The five scans were processed and the step heights for each leg calculated. A plan view of the combined and filtered point clouds used to determine the step heights is shown in Figure 8. The robot was then instructed to take a step forward, and this operation repeated until the robot had moved across the stepfield, as shown in Figure 7 c) and d).

VII. Results and Discussion

The robot was able to make its way over all the tasks set for it only using the leg reflexes. Each time a leg reflex was triggered the CPU load on the myRio increased from 20% to more than 50% to process the reflex. The robot was not able to walk up an incline greater that 20°, before the robot lost traction or one of the rear motors would fail due to over loading. The robot currently only operates with the tripod gait. If the robot could transition to a wave gate then the rear legs would not be carrying this high load and it may be possible to climb a steeper slope. When the robot was making its way over the stepfield, the robot body roll and pitch was maintained to within an angle of 2°, until a foot slipped off of the side of

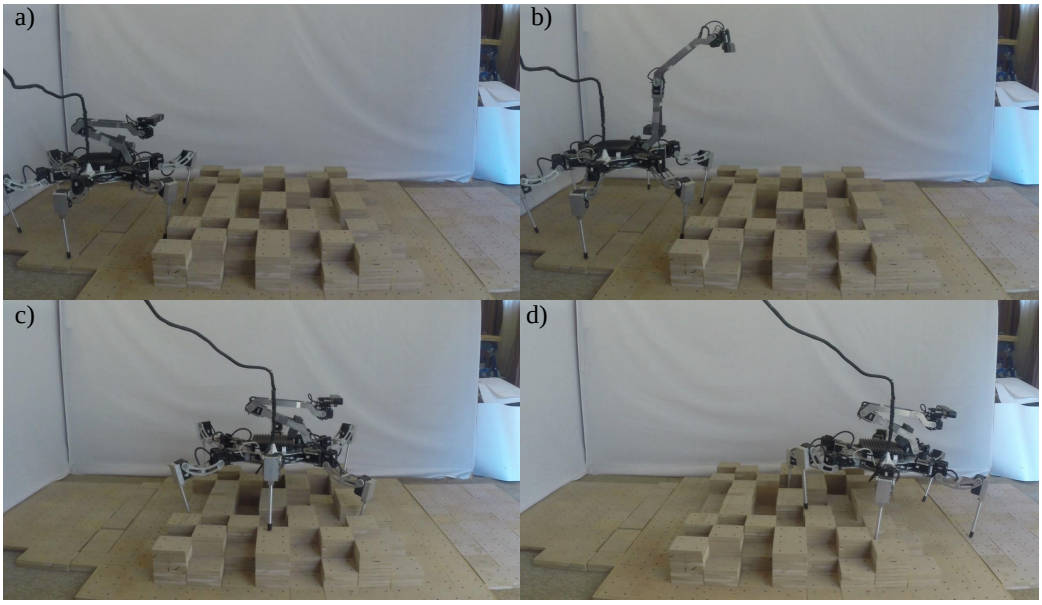

Fig. 7. Robot taking a scan of the stepfield and then walking over the terrain ahead of it

Fig. 8. Plan view of the combined and filtered point clouds

a block the robot had to then find its footing. The maximum recorded body roll or pitch while crossing the stepfield was 6°.

When the vision assisted walking system was incorporated on top of the leg reflex system, the robot was able to make its way across the stepfield without any of the legs making contact with the side of any of the block in the stepfield. For the first test run across the stepfield it was noted that the step trajectory produced a conservative walk pattern as the foot path was some distance away for the blocks. This resulted in the Seek Down Reflex being called and the robot spending time driving the legs down to find a footing. This conservative walk pattern was the result of the interaction between the body levelling and the step trajectory algorithms. The body levelling code was then modified to produce a step trajectory that followed the terrain more closely. The test was then rerun and each step trajectory produced a foot path that required very little use of the Seek Down Reflex. Figure 9 a) is a snapshot of the robot with Leg 2 at the end of a step, and the Seek Down reflex is starting the downward motion for the conservative walk across the stepfield. This is compared in snapshot Figure 9 b) to the position of the foot of Leg 2 with the modified code in operation.

There are two noteworthy advantages for having the step trajectory follow the terrain as closely as possible. The first is the reduction in the time required to walk across the stepfield. Figure 10 shows the respective times to walk across the stepfield for each of the three test types, in bar chart form. The first bar indicates the blind walk test time, and the middle and last bars represent the times for the conservative vision assisted walk and the vision assisted walk with the terrain following code, respectively. It can be seen from the chart that the vision assisted tests were considerably faster than the blind walking test. The time difference between the blind walk test and the modified code run was 4:57 or 53% faster. For the two vision assisted tests, the walk time for the modified code test was 38 seconds or 17% faster. The respective scan times for these two tests cannot be compared directly, as the vision node for the conservative vision test unexpectedly crashed during the scan processing stage of that test. The Point Cloud Library (PCL) [15] integration in ROS was noted to not be very stable. However, the scan and processing times for these two test

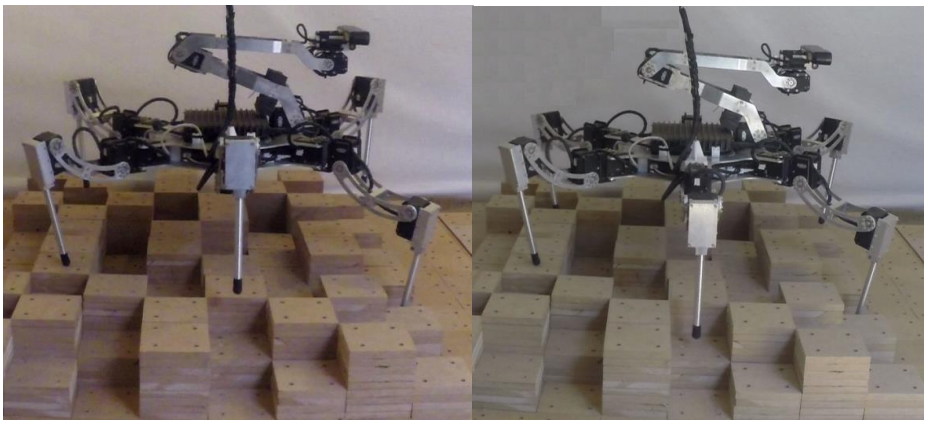

a) b)

Fig. 9. Snapshots showing the start of the Seek Down reflex for Leg 2 for a) conservative step height and, b) terrain following

should theoretically be the same or very similar. The second is the reduction in CPU load. The more time spent processing any of leg reflex routines, the more the myRio CPU is running at the higher load.

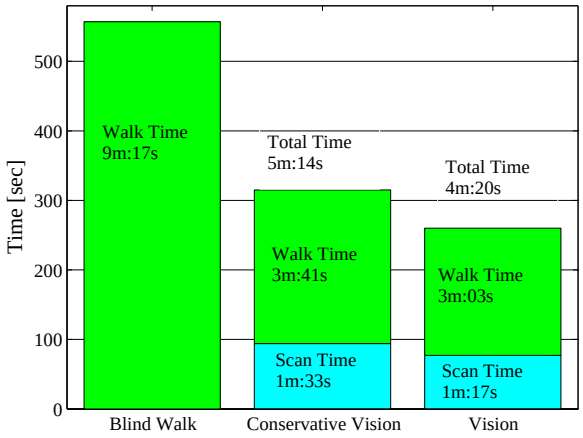

Fig. 10. Time comparison between the blind walk test and the two vision assisted tests

VIII. Conclusions and Future Work

The results of the testing showed that the robotic system developed is capable of tackling a wide range of obstacles by only utilising the reflexes developed. When the vision system was added and used in conjunction with the reflexes, the hexapod was able to make its way across the stepfield considerably faster.

Moving forward for this work the vision system is to be optimized, as currently all processing is done in a serial manner. This will reduce the time from the start of the scan to when that robot can start walking. Stability of the vision system also requires more work. This will include looking at how the PCL is incorporated into ROS. The walk pattern generator for the robot is to be expanded to include the ability of the robot to transition between walk gaits dependant on the terrain ahead of it.

References

[1] A. Simpkins and C. Simpkins, "Rescue Robotics", *Robotics and Automation Magazine*, IEEE, 2014, Volume: 21, Issue: 4.

[2] R. Murphy, "Trial by fire [rescue robots]", *Robotics and Automation Magazine*, IEEE,2004, Volume: 11, Issue: 3.

[3] J. Casper and R. Murphy, "Human-robot interactions during the robot-assisted urban search and rescue response at the World Trade Center", *Systems, Man, and Cybernetics, Part B: Cybernetics*, IEEE, 2003, Volume: 33, Issue: 3.

[4] R. Murphy, "Rats, Robots, and Rescue", *Intelligent Systems*, IEEE, 2002, Volume: 17, Issue: 5.

[5] K. Nagatani, T. Nishimura, and Y. Hada "Redesign of rescue mobile robot Quince", *Proceedings of the 2011 IEEE International Symposium on Safety,Security and Rescue Robotics*, Kyoto,Japan,November 1-5 2011.

[6] M. H. Raibert,"Legged Robots", *Communications of the ACM*, Volume. 29, 1986.

[7] D. C. Kar, "Design of a statically stable walking robot: A review", *Journal of Robotic Systems*, Pages: 671686, 2003.

[8] T. Booysen and S.T. Marais, "The development of a remote controlled, omnidirectional six legged walker with feedback" *AFRICON*, 2013

[9] A. R. Hevner, S. T. March, J. Park, and S. Ram. "Design science in information systems research". MIS Quarterly, 28:75105, 2004.

[10] M. A. Chace. "Vector Analysis of Linkages". *Journal of Engineering for Industry*,(289-297), 1963

[11] K. S. Espenschied, R. D. Quinn, R. D. Beer, and H. J. Chiel. "Biologically based distributed control and local reflexes improve rough terrain locomotion in a hexapod robot". *Robotics and Autonomous System*, volume 18, pages 5964, 1996.

[12] J. Mrva and J. Faigl. "Tactile Sensing with Servo Drives Feedback only for Blind Hexapod Walking Robot". *Proceedings of the 10th International Workshop on Robot Motion and Control*, IEEE, 2015.

[13] D. Gouaillier, V. Hugel, and P. Blazevic, "Mechatronic design of NAO humanoid", *International Conference on Robotics and Automation*, IEEE, Pages: 769 - 774, 2009.

[14] H. Zhang, Y. Liu, J. Zhao, J. Chen, and J. Yan. "Development of a Bionic Hexapod Robot for Walking on Unstructured Terrain", *Journal of Bionic Engineering*, Volume:11, 2014.

[15] R. Rusu and S. Cousins. 3D is here: Point Cloud Library (PCL). In ICRA Communications, IEEE, 2011.